ELSEVIER

Polymer 41 (2000) 1355–1368

polymer

Characterization of ultra high molecular weight polyethyelene nascent reactor powders by X-ray diffraction and solid state NMR

Y.L. Joo[a,1,*], O.H. Han[b,2], H.-K. Lee[a,1], J.K. Song[a,1]

[a]*Hanwha Group Research and Engineering Center, 6 Shinsung-dong, Yusung-ku, Daejeon 305-345, South Korea*
[b]*Korea Basic Science Institute, 52 Yeoeun-dong, Yusung-ku, Daejeon 305-333, South Korea*

Received 7 January 1999; received in revised form 15 March 1999; accepted 31 March 1999

Abstract

The nascent ultra-high molecular weight polyethylene (UHMWPE) reactor powders are prepared by polymerizing ethylene in the presence of soluble magnesium complexes under various reaction conditions. It is found that the polymerization process applied in the study provides a high yield of UHMWPE even at low polymerization temperature, and the reactor powders exhibit high melting temperatures (137–143°C) and heat of melting (180–210 J/g). X-ray diffraction (XRD) patterns and solid state ^{13}C magic angle spinning (MAS) NMR spectra of the powders synthesized under various reaction conditions are examined and compared with those of a commercial UHMWPE powder. Our results reveal that a significant portion of the monoclinic phase is identified when the resin is polymerized at relatively low temperatures. Temperature dependent XRD and NMR experiments show that UHMWPE reactor powders synthesized in the study exhibit more drastic thermal behaviors than the commercial UHMWPE, and this difference becomes more pronounced with the reactor powders polymerized at low temperatures. The increased crystallinity and crystal size in newly synthesized UHMWPE powders at elevated temperatures (100–125°C) may significantly improve the processability of UHMWPE reactor powders into high strength tapes below their melting temperature.

Keywords: Ultra-high molecular weight polyethylene synthesis; X-ray diffraction; Solid state NMR

1. Introduction

Commercial ultra-high molecular weight polyethylene (UHMWPE), a polymer with a very high degree of polymerization, is generally produced by the low-pressure Ziegler process with organometallic catalysts [1]. Meanwhile, as-polymerized or nascent, crystallizable UHMWPE has been a topic of interest in developing solvent-free routes to high modulus, high strength polyethylene products [2–7]. It was recognized that under certain experimental conditions monomers might simultaneously polymerize and crystallize into non-entangled conformation. The UHMWPE films were produced by depositing a vanadium catalyst system on glass slides, followed by polymerization of ethylene at relatively low temperatures [2–4] or nascent UHMWPE reactor powders were synthesized at low temperature in the presence of SiO_2-supported vanadium catalyst system [5]. These methods, however, lack industrial significance because the yield of polymerization is not high enough. Moreover, the past research on UHMWPE synthesized at relatively low temperatures has concentrated mostly on the solid state drawing characteristics [2–7], while the structure of such polymers is seldom studied rigorously.

The present report describes an attractive route to UHMWPE powder synthesis of nascent UHMWPE under conditions where the macromolecules are produced directly in an untangled conformation. The characteristics of UHMWPE reactor powders synthesized under various temperatures and pressures are presented in this study. Polymerization of ethylene in the presence of soluble magnesium complexes at low temperatures provides high yield values [8]. We will demonstrate that such as-polymerized polyethylenes exhibit a number of properties that are remarkable in comparison with those of the once-molten (and re-entangled) polyethylene: a very high crystallinity, high melting temperature, and sufficiently large micropore volumes and inner surface areas. As a result, the

* Corresponding author. 66-250 Department of Chemical Engineering, Massachusetts Institute of Technology, Cambridge, MA 02139, USA. Tel.: +1-617-253-6547; fax: +1-617-258-8992.
E-mail address: yongjoo@mit.edu (Y.L. Joo)
[1] Tel.: +82-42-865-6558; fax: +82-42-865-6570.
[2] Tel.: +82-42-865-3436; fax: +82-42-865-3419.

0032-3861/00/$ - see front matter
PII: S0032-3861(99)00272-4

Table 1
Characteristics of UHMWPE nascent reactor powders under various polymerization conditions

Sample code	[Mg] (g/l)[a]	T_{pol} (°C)[b]	P_{C2H4} (psig)[c]	Y (Kg PE/gTi h atm)[d]	M_v ($\times 10^6$)[e]	T_m (°C)[f]	ΔH_f (J/g)[g]
GUR412	–	–	–	–	2.4	141.6	170
10C_15P	4.0	10	15	7	2.7	141.6	208
30C_15P	2.5	30	15	212	1.8	141.5	195
45C_15P	2.5	45	15	230	1.7	141.6	178
60C_15P	2.5	60	15	214	1.0	140.5	184
90C_15P	2.5	90	15	108	0.6	136.6	191
30C_40P	1.25	30	40	250	3.8	143.4	184
90C_40P	1.25	90	40	164	0.5	138.6	192

[a] [Mg] is the concentration magnesium.
[b] T_{pol} is the polymerization temperature.
[c] P_{C2H4} is the ethylene pressure.
[d] Y is the yield.
[e] M_v is the molecular weight from intrinsic viscosity.
[f] T_m is the melting point.
[g] ΔH_f is the enthalpy of fusion.

polymerized reactor powder can readily be compacted below its melting point and drawn into high-strength films or filaments without further treatment.

After examining the thermal properties and morphology of newly synthesized UHMWPE reactor powders, X-ray diffraction patterns and solid state ^{13}C NMR spectra of the powders synthesized under various reaction conditions are studied to probe the crystalline and amorphous phase structures and compared with those of a commercial UHMWPE powder.

It is well known that the monoclinic phase of linear polyethylene is formed when the polymer is subjected to stress beyond the yield point, while the monoclinic phase has also been identified in low temperature reactor powders, which were not subject to stress in the usual macrscopic sense [9]. The monoclinic phase is known to seldom constitute more than ten percent of the total crystalline content of polymer. On the contrary, a significant portion of the monoclinic phase is identified by both wide angle X-ray diffraction and solid state NMR spectroscopy in our newly synthesized UHMWPE reactor powders when polymerized at relatively low temperatures. It is also found that the fraction of monoclinic phase depends sensitively on the polymerization temperature. Temperature-dependent WAXS and NMR experiments were carried out to examine the influence of temperature on crystalline structures: the results show that our samples exhibit quite different thermal behaviors from the commercial UHMWPE powder.

Furthermore, the dynamics of carbon atoms in each phase were compared by measuring the ^{13}C spin–lattice relaxation times (T_1), ^{13}C spin–spin relaxation times (T_2), and cross polarization (CP) times (T_{CH}), and the significant portion of intermediate phase with a *trans*-conformation but the higher chain mobility than crystalline phases is identified.

2. Experimental

2.1. UHMWPE synthesis [8]

2.1.1. Magnesium-organic catalyst

Into 1 l glass reaction flask 15 g metallic magnesium, 60 ml *n*-heptane, 5 ml 1-chlorobutane and 6 mmol triethylaluminium (TEAL) were charged in a nitrogen atmosphere. Thereafter temperature was raised to a boiling point of the mixture and stirring for 20 min. Subsequently, 54 g 1-chlorobutane in solution of *n*-heptane (440 ml) was drop-wise introduced into the reactor flask. After heating the mixture for 2 h 0.195 mol TEAL was charged into the reactor and heated for 1 h. After precipitation of the residues, the

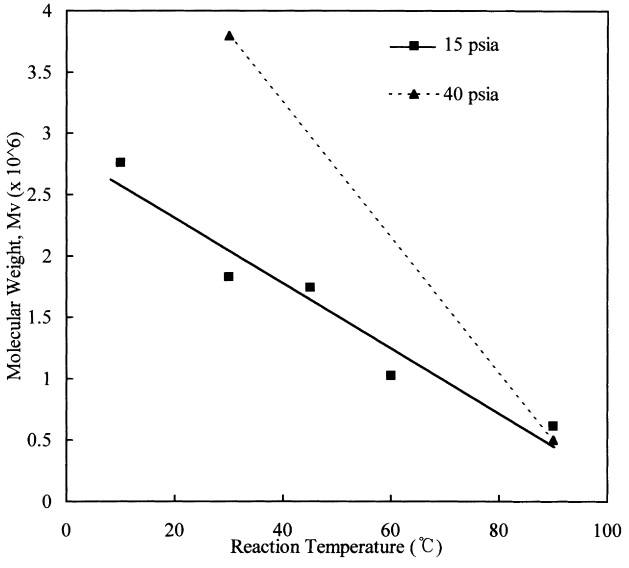

Fig. 1. Molecular weight vs. reaction temperature. Molecular weight of UHMWPE powders synthesized under various conditions is obtained from the intrinsic viscosity measurements.

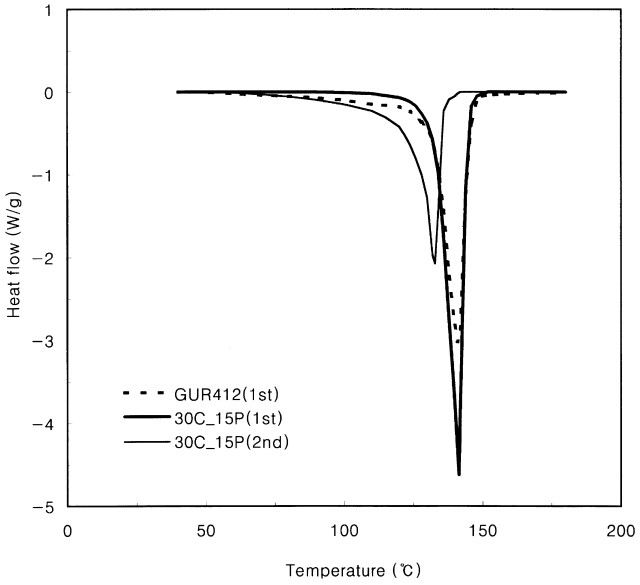

Fig. 2. Differential scanning calorimetry curves of the two subsequent melting runs for a typical UHMWPE reactor powder, 30C_15P. The curve of GUR412 is also shown for comparison.

supernatant clear liquid part, which contained 7.4 g/l of magnesium, was used as the soluble magnesium-organic component of the catalyst system in the polymerization of UHWMPE.

2.1.2. Polymerizations

Into a 20 l slurry reactor 10 l of *n*-heptane, 6 ml solution of TEAL (1M solution in heptane), 88 ml solution of the magnesium-organic soluble component, 90 mg tetrahydrofurane, 6.4 g diethylaluminium and then 29 mg titanium tetrachloride in ethylene atmosphere were charged. Polymerization was conducted for 1 h at five different polymerization temperatures (10–90°C) and two ethylene pressures (1 and 3 atm). Some characteristics of the newly synthesized UHMWPE powders are listed and compared with a commercial UHMWPE powder, Hostalen GUR412, in Table 1. Hostalen GUR412 was provided by the manufacturer (Hoechst AG), and it is known to be polymerized by the low-pressure Ziegler process at relatively high temperatures with organometallic catalyst similar to that for conventional high density polyethylene (HDPE) [1].

2.2. Characterization

2.2.1. Molecular weight

Molecular weight of each sample was estimated from its intrinsic viscosity in decalin at 135°C measured at Automatic Viscometer, AUTOVISC I, by Cannon; the three polymer concentrations applied were 0.05, 0.1, and 0.15 g/l, respectively. The intrinsic viscosities of all samples were in the range of 6–25 dl/g which correspond to average molecular weights of $0.5–4 \times 10^6$.

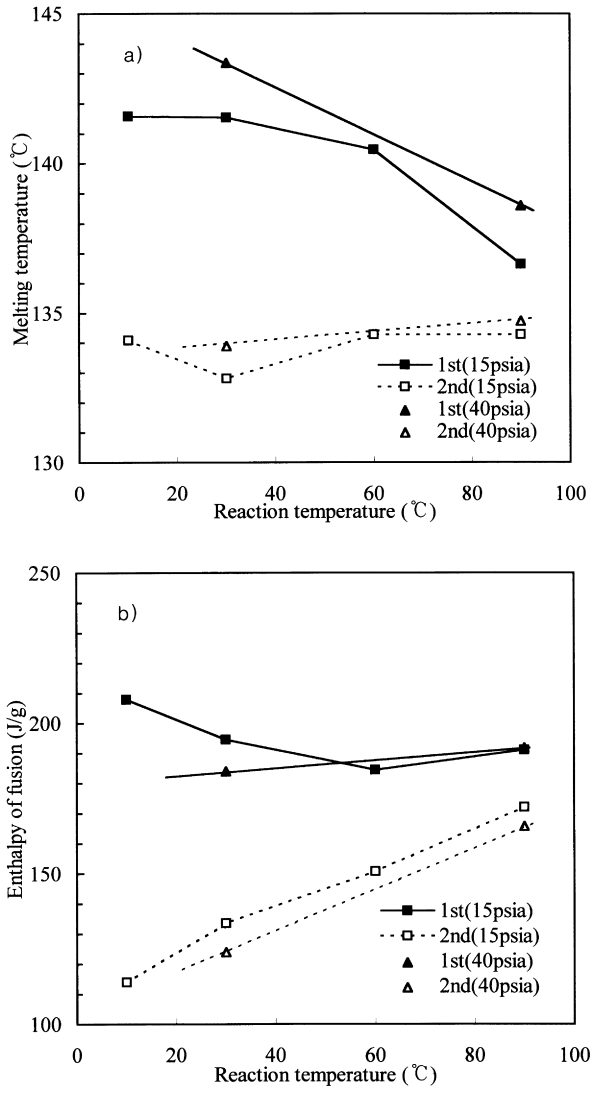

Fig. 3. Thermal behaviors of UHMWPE powders of the two subsequent melting runs with differential scanning calorimetry: (a) melting temperature; and (b) heat of fusion vs. reaction temperature are plotted.

2.2.2. Thermal properties

Each sample (weight of about 5 mg) was set in a DSC apparatus (DuPont 2100). The melting peak temperature and heat of fusion of each sample was measured at the heating rate of 10°C/min. After the first run, each sample was cooled and the scan was carried out at the same heating rate to determine the differences in both melting temperature and heat of fusion between the two subsequent melting runs.

2.2.3. X-ray diffraction experiments

Powder X-ray diffraction measurements were done on a diffractometer by Material Analysis and Characterization, using nickel-filtered CuKα radiation ($\lambda = 0.15406$ nm) operating at 45 kV and 100 mA. The diffractometer was equipped with Soller slits in both the incident and reflected

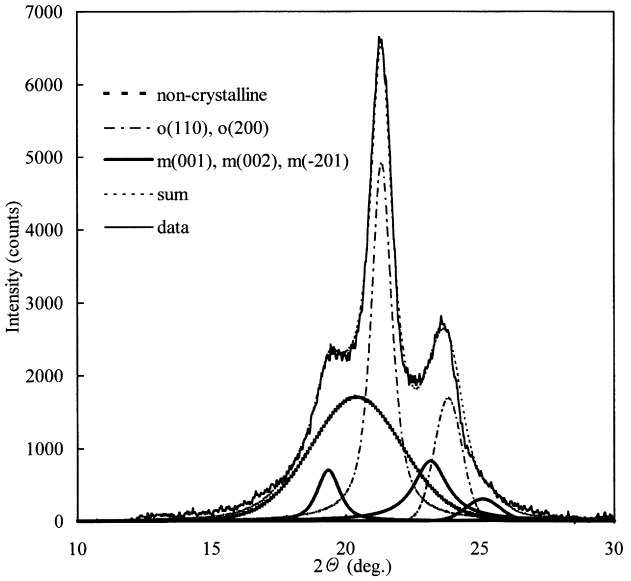

Fig. 4. Deconvolution of the WAXS pattern of a typical UHMWPE powder into three different contributions from: (a) non-crystalline; (b) orthorhombic crystalline; and (c) monoclinic phases.

beams. The data were collected in the 2θ range of 15–40°, in steps of 0.04° and a scanning rate of 4 s per point. The profile fit/deconvolution program employed to analyze the patterns can be found elsewhere [10–11]. Crystallite size was calculated from the integrated WAXS line width using the Scherrer equation, after correction for instrumental and Kα doublet broadenings was made. Powder X-ray diffraction as a function of temperature was also measured to probe the thermal behaviors of the samples. The powders were packed into an aluminum sample container ($20 \times 12 \times 1$ mm^3) which was mounted on a sample stage consisting of a tantalum heating strip. Temperature was recorded by a Chromel–Alumel thermocouple inside the sample container. Temperature was controlled by another thermocouple, welded on the back of the tantalum strip. The temperature error was estimated to be about 1°C.

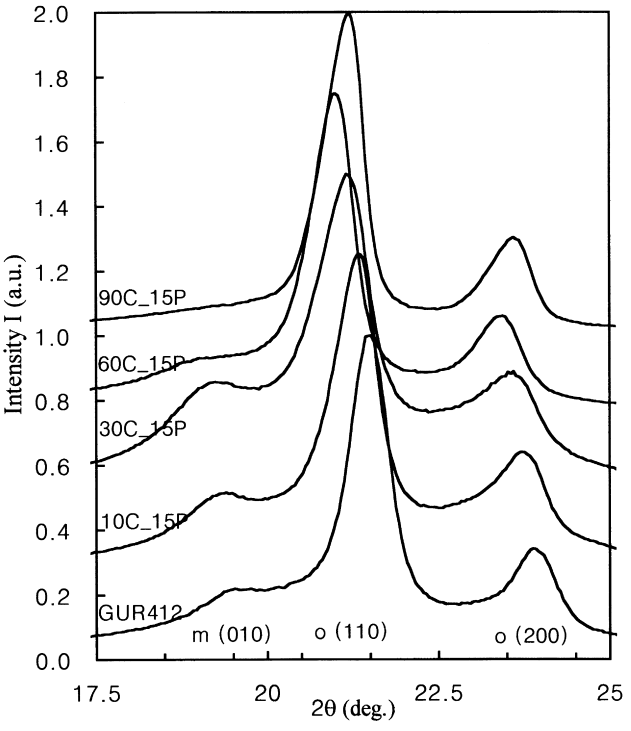

Fig. 5. The room temperature WAXS patterns of various UHMWPE powders synthesized under various conditions. That of GUR412 is also shown for comparison.

2.2.4. Solid State NMR spectroscopy

Solid state NMR spectra were obtained using a DSX 400 (Bruker Analytik GmbH, Germany). High-power proton decoupling and magic angle spinning (MAS) but without CP was applied to determine the mass fractions of phase components in each powder sample. The decoupling strength was 65.8 kHz and the decoupling method of tppm [12] was used. The spinning speed was 10.0 ± 0.005 kHz. Temperature dependent CP/MAS NMR experiments from 25 to 120°C were carried out to observe the relative variation in morphology. Proton power for CP was the same with decoupling power. T_1 was measured with Torchia's pulse sequence [13] and T_2 was determined from dipolar dephasing rate after CP. The CP rate was also compared for the study of dynamics in each phase.

3. Results and discussion

3.1. Characteristics of UHMWPE powders

The basic properties of UHMWPE powders synthesized under various reaction conditions are listed in Table 1 where the sample code, GUR412, denotes a commercial UHMWPE powder "Hostalen GUR412" (Hoechst AG) and the others denote the newly synthesized UHMWPE powders. The samples are named as follows: for example, in 10C_15P, the former 10C and the latter 15P denote the polymerization temperature of 10°C and the ethylene pressure of 15 psi, respectively.

We note that the polymerization of ethylene could not be proceeded without adding soluble magnesium-organic component of catalyst system under the reaction conditions studied. The yield of most UHMWPE powders ranged from 100 to 250 kg of PE/(gTi h atm). It is observed that the yield drops significantly at temperatures below 20°C and increases with increasing ethylene pressure.

The molecular weight which was obtained from the intrinsic viscosity measurements of UHMWPE powders polymerized under various conditions are depicted in Fig. 1. The molecular weight gradually decreases as the polymerization temperature increases at the same catalyst concentration and ethylene pressure. As a result, the molecular weight becomes below 10^6 at high polymerization temperature (90°C). Meanwhile, in our solution ^{13}C NMR

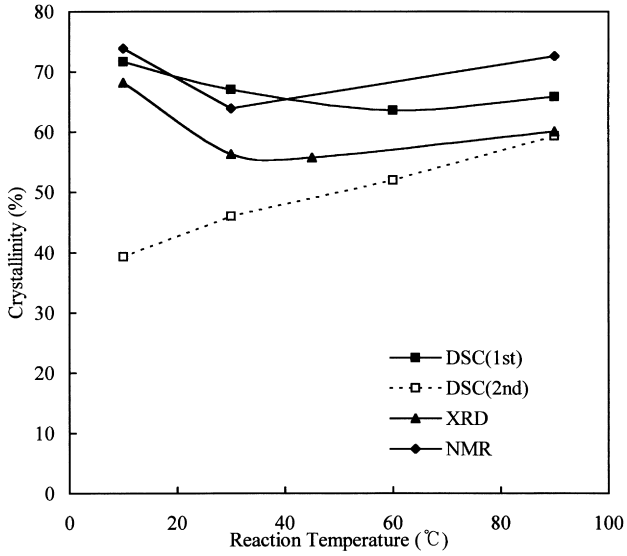

Fig. 6. The crystallinity of UHMWPE reactor powders vs. polymerization temperature determined by calorimetry, X-ray diffraction, and solid state NMR. The powders considered here are all polymerized at the same ethylene pressure (15 psia).

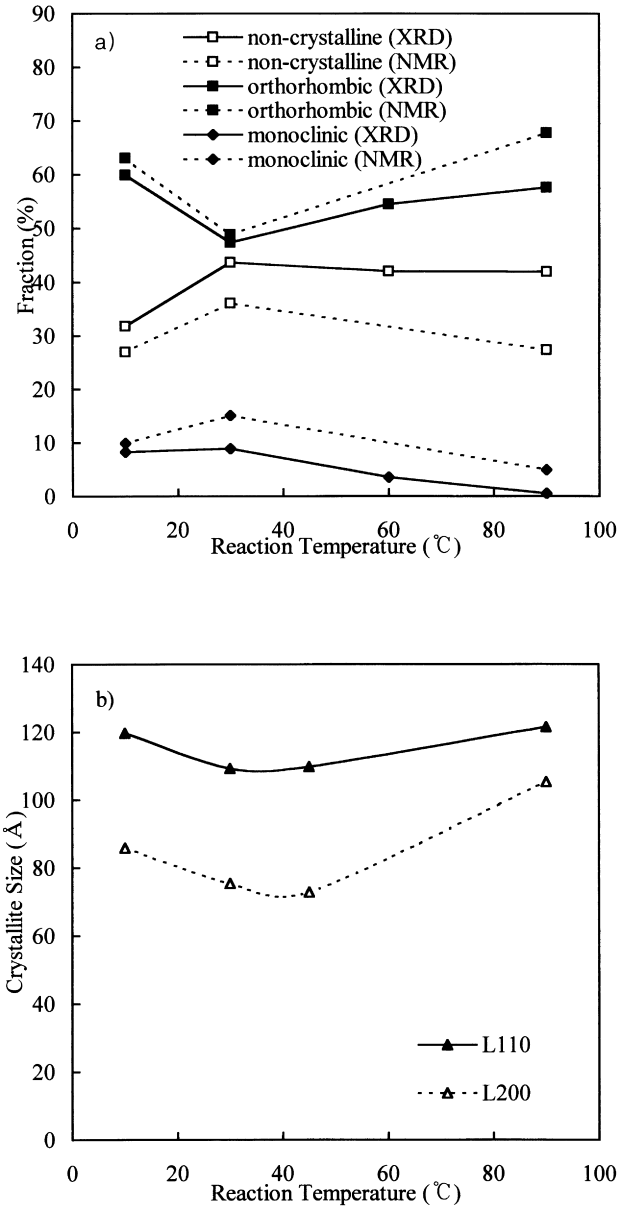

Fig. 7. Reaction temperature dependence of: (a) phase composition; and (b) orthorhombic crystallite size determined from the X-ray diffraction patterns of various UHMWPE powders synthesized under various temperatures (at 15 psia). The phase composition obtained from the solid state ^{13}C MAS NMR experiments is also shown for comparison.

experiments show that the UHMWPE molecules synthesized in this study are found to have very low contents of side chains, which makes it possible to consider them as ideal two-ended long molecules with no side chains.

In Fig. 2, schematic illustration of differential scanning calorimetry is presented. The heating curve for the UHMWPE powder in this study is characterized by a narrow and sharp fusion peak, and the melting becomes noticeable from 125°C. On the contrary, the onset of the melting for GUR412 is found to take place at a much lower temperature of 60°C despite very close melting peak temperatures in two samples. The melting peak temperature and heat of fusion of the UHMWPE powder in the second melting run are significantly reduced after rapid cooling. It is also observed that in the second melting run the melting starts at lower temperature and the fusion peak becomes broader.

The reactor powders exhibit high melting temperatures (137–143°C) and heat of melting (180–210 J/g) as shown in Fig. 3. The melting temperature obtained from the first melting run gradually increases as polymerization temperature is decreased. We note that higher molecular weight UHMWPE powder polymerized at low temperature exhibits higher melting temperature and heat of fusion than those polymerized at high temperatures. This may be due to a high ordering (non-entangled conformation) of the crystal phase upon polymerization and crystallization at low temperatures [2–7]. We can easily surmise that such a non-entangled conformation becomes less favorable with increasing polymerization temperature. Later, we will demonstrate that such high melting temperature and heat of fusion for UHMWPE reactor powders synthesized at low temperatures are also associated with thermally induced changes in crystalline phases via our temperature-dependent X-ray diffraction and solid state NMR results.

On the contrary, the melting point and heat of fusion gradually increases with increasing polymerization temperature in the second melting run. Once UHMWPE nascent reactor powders are melted, and therefore non-entangled conformation is destroyed, chain entanglements of high molecular weight molecules take place favorably. The entanglements effectively depress crystallization of large portions of the molecules, leading to lower crystallinity [14–16]. As a result, each reactor powder exhibits a remarkable difference in melting temperature and heat of

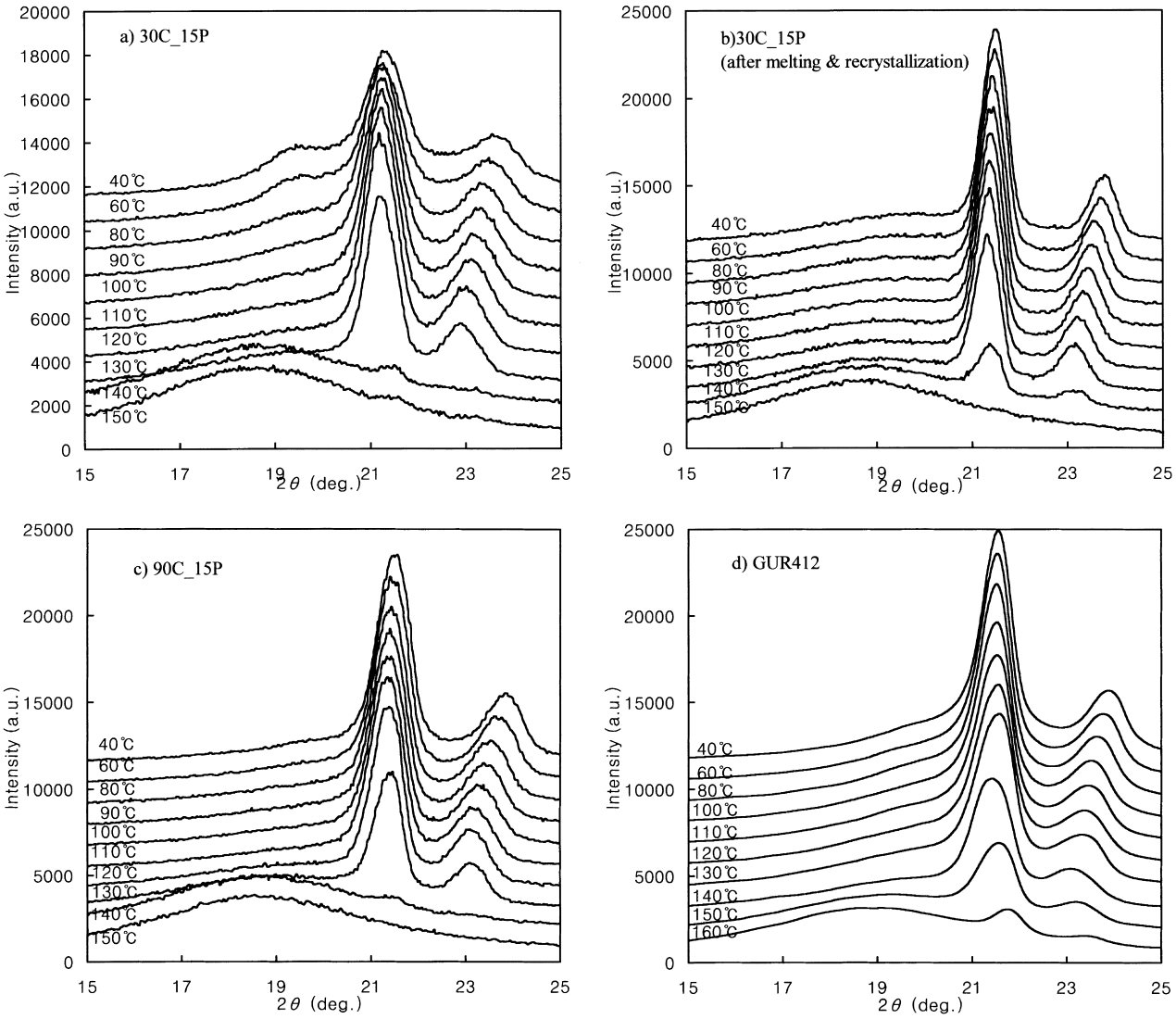

Fig. 8. Temperature-dependent XRD patterns for various UHMWPE powders: (a) 30C_15P; (b) 30C_15P after melting and recrystallization; (c) 90C_15P; and (d) GUR412.

melting determined under two subsequent melting runs especially for the powders synthesized at low temperatures as shown in Fig. 3.

In a later report, we will demonstrate that UHMWPE reactor powders synthesized in this study also have a distinct morphology characterized by a low bulk density, high micropore volume and inner surface area, and these properties provide a successful continuous production of high strength, high modulus materials at a temperature below their melting points [17].

3.2. X-ray diffraction studies

Wide angle X-ray scattering (WAXS) analysis was conducted to probe the crystal phase structures of UHMWPE powders. We can easily surmise that the UHMWPE molecules synthesized at relatively low temperatures exhibit different phase structures from the commercial UHMWPE prepared by the low-pressure Ziegler process. Therefore, the focus of these experiments is on the determination of structural differences between a commercial UHMWPE powder and newly synthesized UHMWPE powders under various polymerization conditions.

The WAXS diffraction pattern of a typical UHMWPE reactor powder synthesized at low temperature is illustrated in Fig. 4. As seen in the figure, the diffraction peaks observed were the monoclinic (001) reflection, and the orthorhombic (110) and (200) reflections; a broad non-crystalline halo was also observed [9]. The predominating crystalline form for all the samples is the orthorhombic form, characterized by the peaks at 21.5 and 23.8°. Only one reflection at 19.4° is a clear evidence for the presence of the monoclinic form: the other two monoclinic reflections are severely overlapped with the second orthorhombic reflection [9]. We followed the X-ray diffraction analysis

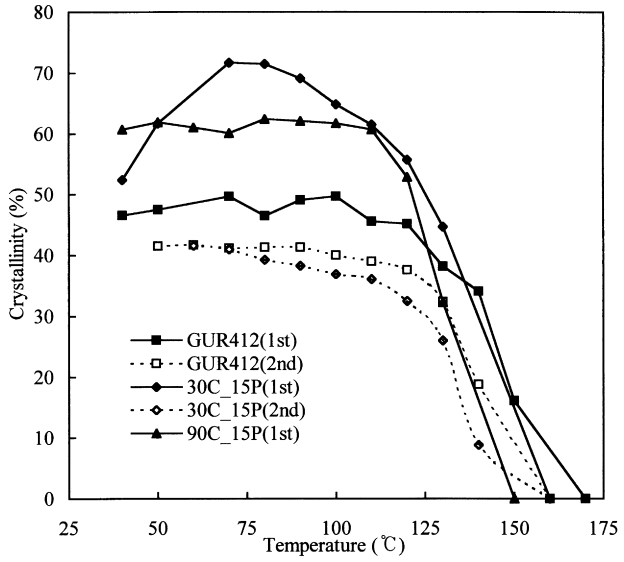

Fig. 9. Thermal behaviors of various UHMWPE powders in the X-ray diffraction: the crystallinity vs. measuring temperature is shown.

by Russell et al. [9], and the deconvolution of the WAXS pattern into three different contributions from non-crystalline, orthorhombic, and monoclinic phases is also shown in the figure.

We note that a significant portion of the monoclinic phase (10–20% of the total crystalline content of polymer) is identified in the newly synthesized UHMWPE powders polymerized at relatively low temperatures (30C_15P). It is found that the fraction of monoclinic phase decreases with increasing polymerization temperature, and the monoclinic phase is hardly observed when the powder was polymerized at 90°C (see Fig. 5). Therefore, it can be concluded that the formation of the monoclinic crystalline phase depends strongly on the polymerization temperature in our UHMWPE synthesis.

It should also be noted that the peak positions of the orthorhombic (110) and (200) reflections move to the left and then to the right along the $x(2\theta)$-axis as polymerization temperature increases. As a result, the largest orthorhombic subcell (unit cell) sizes of the *a,b* plane of the orthorhombic reflections are obtained for the UHMWPE powder polymerized at 60°C.

The degree of crystallinity determined by calorimetry and X-ray diffraction analysis are plotted against polymerization temperature in Fig. 6. The crystallinity obtained from ^{13}C solid state NMR in the following section is also plotted for comparison. It is observed that the crystallinity from XRD analysis is lower than that from the calorimetry, although its dependence on polymerization temperature is in qualitative agreement. We note that XRD experiments are carried out at 25°C and thus the XRD results represent the crystallinity at the state of non-entangled conformation, while the calorimetry may involve certain conformational changes during the measurement due to heating. The changes in the crystal phases are inevitable because of the presence of the

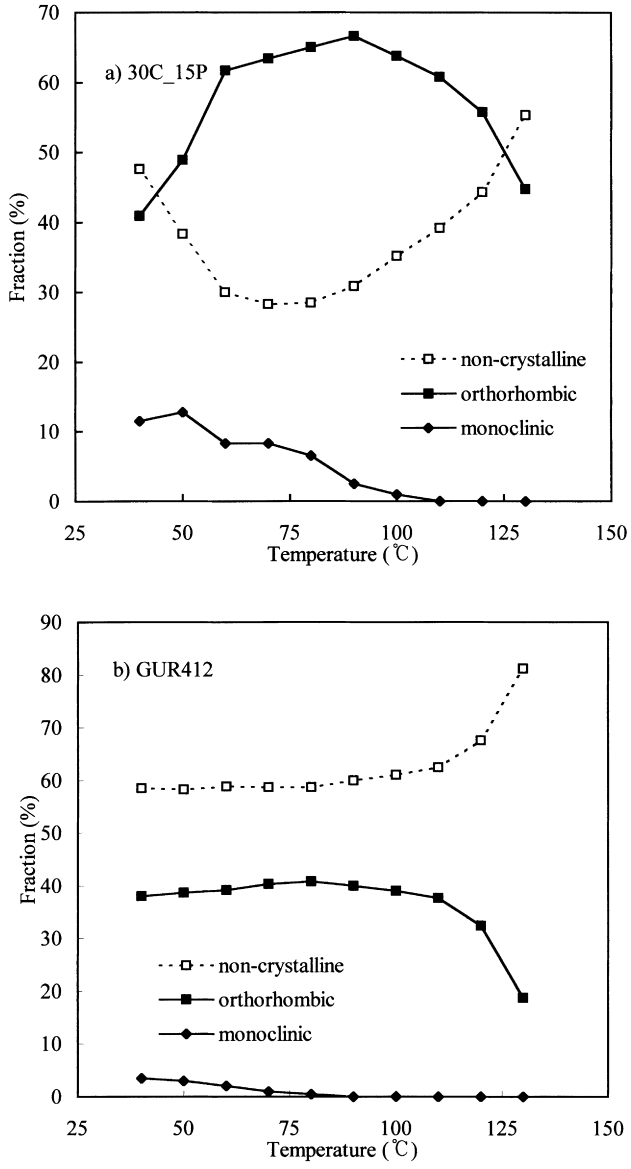

Fig. 10. Phase composition plots from X-ray diffraction patterns of each sample at various temperatures: (a) 30C_15P; and (b) GUR412.

monoclinic phase in the powders polymerized at low temperatures. It was reported previously that the monoclinic peak starts decreasing in intensity at about 80°C in their temperature-dependent XRD experiments [18]. It is noticeable that the difference in the crystallinity from both methods is greater as the monoclinic phase of the total crystalline content is increased.

The dependence of the phase composition on the polymerization temperature can be seen in Fig. 7(a). The results obtained from the solid state ^{13}C NMR are also plotted for comparison. It is observed that the orthorhombic portion initially decreases with increasing reaction temperature, but it starts to increase as the monoclinic portion is decreased at higher temperature. Meanwhile, the non-crystalline portion increases with polymerization temperature and reaches a steady value (~40%) at polymerization

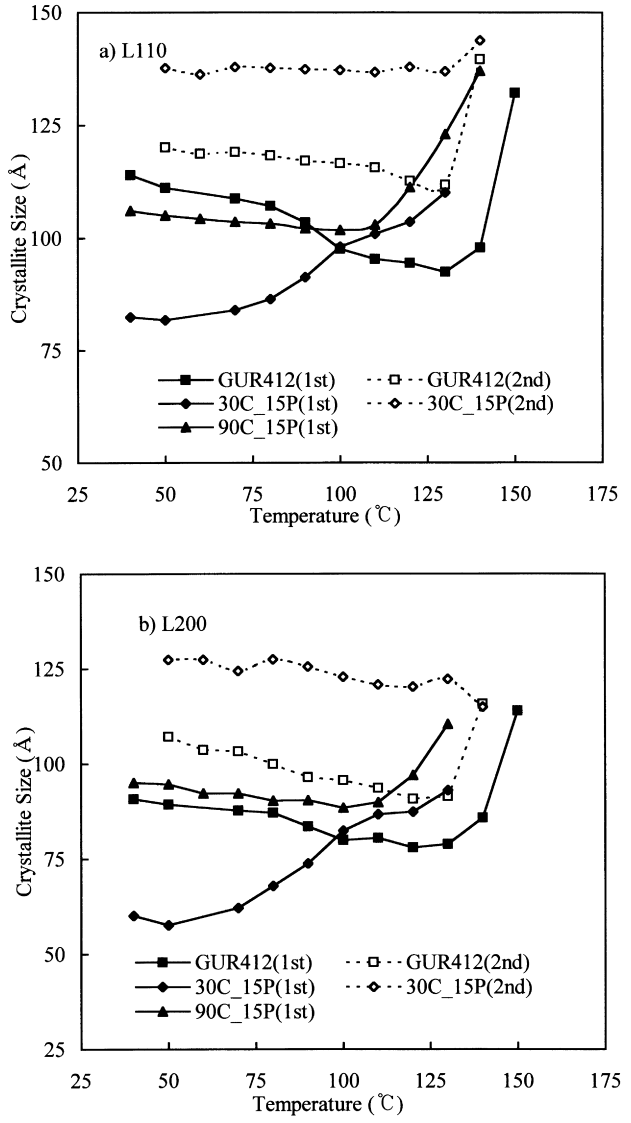

Fig. 11. The average crystallite dimensions perpendicular to the orthorhombic (200) and (110) planes vs. measuring temperature for various UHMWPE powders.

temperature $T_{pol} > 30°C$. It should also be noted that the average crystallite dimensions perpendicular to the orthorhombic (200) and (110) planes decrease with increasing polymerization temperature, but start to increase as the monoclinic phase is reduced. They are estimated to vary from 110 to 125 Å and from 70 to 105 Å, respectively (see Fig. 7(b)).

To investigate the thermal behavior of each phase in UHMWPE powders, X-ray diffraction as a function of temperature was also measured and illustrated in Fig. 8. It is observed that the monoclinic peak of the UHMWPE powder polymerized at low temperature (30C_15P) decreases in intensity as temperature increases and disappears above 100°C indicating the loss of the monoclinic phase. It is also observed that as temperature increases, the orthorhombic peaks grow up in intensity and their shapes become sharp, which means that the sample has more orthorhombic phase with increasing temperature. This may imply that the evident phase transition from the monoclinic to the orthorhombic takes place as temperature increases. It seems that the required energy to overcome the energy barrier in the phase transition from the monoclinic to the orthorhombic could easily be obtained by heating the sample. After melting and rapid cooling of the same sample, however, the monoclinic phase is absent, and the increase in orthorhombic crystal phase with increasing temperature was no longer observed (Fig. 8(b)). In contrast, the orthorhombic (110) and (200) reflections for GUR412 steadily decreases with increasing temperature as shown in Fig. 8(d).

The temperature dependence of crystallinities of various UHMWPE powders is illustrated in Fig. 9. It is found that the crystallinity of UHMWPE powder polymerized at low temperatures (30C_15P) increases with increasing temperature and drops drastically when the melting takes place. The crystallinity decreases gradually in the second melting run as temperature is elevated after melting and rapid cooling of the same sample. When the fraction of the monoclinic phase in the solid state is small (GUR412 and 90C_15P), however, the crystallinity remains unchanged until the melting of the sample starts.

It should be note that the 2θ values for the maximum of the non-crystalline halo for most UHMWPE powders, $2\theta_{halo}$, is about 20.5–21° which is clearly higher than the value of 19.4° associated with liquid-like amorphous molecules [11]. This implies that there is scattering from some more tightly packed molecules at the solid state hidden under the halo. This issue will be brought up into focus in the solid state ^{13}C NMR studies section. It is observed that $2\theta_{halo}$ values sharply drops to those for liquid low molecular polyethylene upon the completion of the melting procedure, and $2\theta_{halo}$ values of the quenched samples becomes smaller than those of the original reactor powders.

In Fig. 10, the temperature dependence of phase compositions for both 30C_15P and GUR412 is illustrated. The orthorhombic crystalline portion for UHMWPE synthesized at 30°C sharply increases with increasing temperature, while the monoclinic portion steadily decreases. The non-crystalline portion initially decreases and increases at higher temperatures. Meanwhile, the orthorhombic crystalline and non-crystalline portions for GUR412 keep unchanged until the factual melting take place ($T > 100°C$).

The temperature dependence of the average crystallite dimensions perpendicular to the orthorhombic (200) and (110) planes is depicted in Fig. 11. It is found that the orthorhombic crystallite size for the UHMWPE powder prepared at low temperature increases, while those for GUR412 drop with increasing temperature. From the temperature dependence of X-ray diffraction data, it is evident that the thermal phase transitions in the UHMWPE powder synthesized in this study are more drastic than those for the commercial UHMWPE powder, GUR412. We note that the increase of the orthorhombic crystallite size

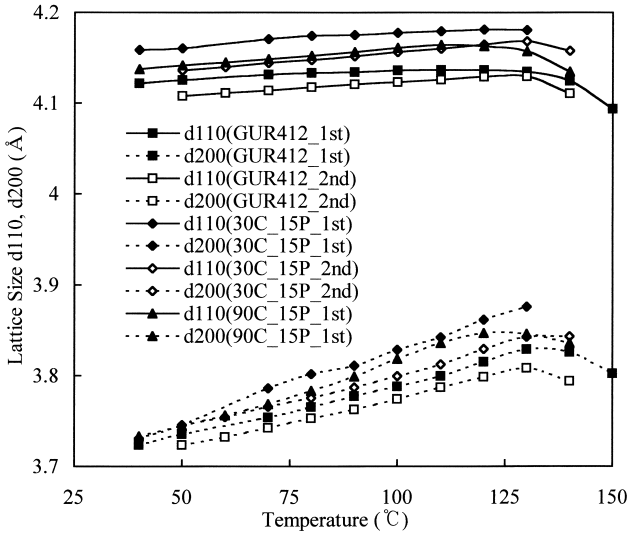

Fig. 12. The temperature dependence of orthorhombic unit cell size in *a*,*b* planes for various UHMWPE powders.

coincides with the reduction of the monoclinic phase. The increase of the crystallinity and orthorhombic crystallite size in the UHMWPE reactor powders prepared at low temperature may imply that the metastable monoclinic phase is transformed into a more stable orthorhombic crystalline phase as temperature is increased.

Finally, the orthorombic subcell sizes in the *a*,*b* plane of UHMWPE powders at various temperatures are shown in Fig. 12. The subcell sizes increase with increasing temperature possibly due to the thermal expansion, and the increase in *a*-axis is more pronounced. In contrast, the subcell sizes decrease after melting and rapid cooling.

3.3. Solid State NMR studies

Our ^{13}C CP/MAS and MAS without CP spectra in Fig. 13 seem to have three main peaks. However, spectrum deconvolution indicates that there is one more component at 33.4 ppm in addition to the well known three peaks [19] from amorphous (at 31.3 ppm), orthorhombic crystalline (at 32.8 ppm), and monoclinic crystalline (at 34.1 ppm) phases as shown in Fig. 14. Analysis of T_1 data has been employed to find out different phases in PE samples in previous reports [20]. We followed the analysis methods by data fitting with peak heights at 32.8 or 34.1 ppm or integrated areas including all signals, which resulted in at least three T_1 values (1000 s, 80 s, and 444–879 ms). According to the previous reports, this implies that there is another component with the middle T_1 value of which the peak is overlapped with those at 32.8 or 34.1 ppm. On the contrary, T_1 data fitting with deconvoluted peak areas reveal that peaks at 32.8 and 34.1 ppm still show double exponential relaxation behavior, while peaks at 31.4 and 33.4 ppm relax in single exponential functions as expected (Table 2). However, data fitting for CP rate and ^{13}C T_2

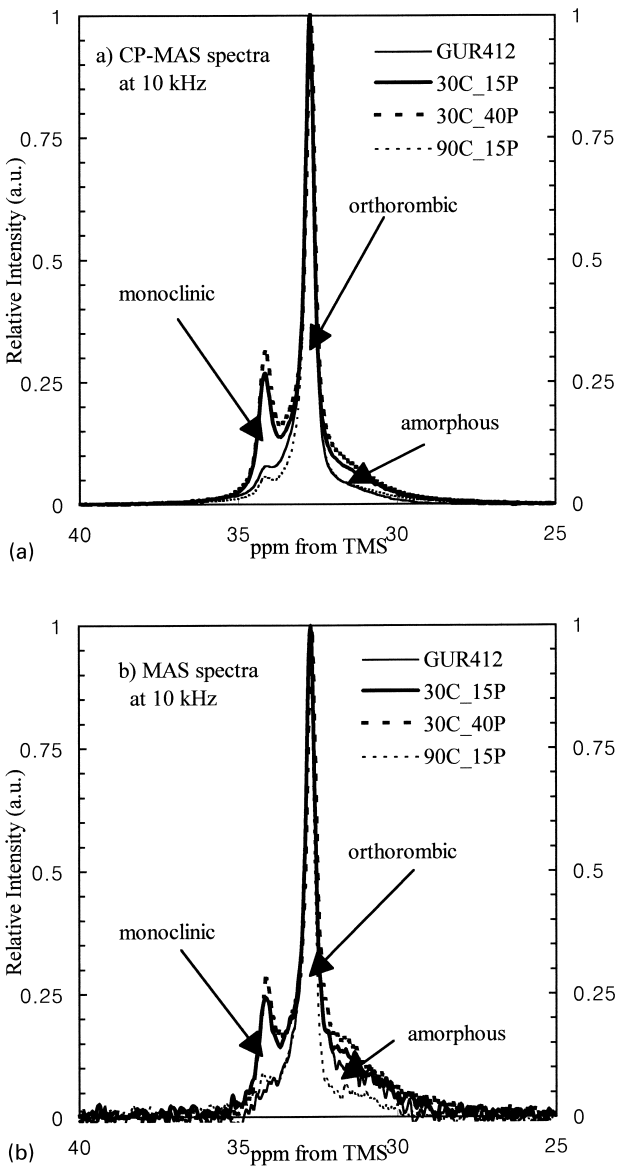

Fig. 13. ^{13}C CP/MAS spectra and MAS spectra of GUR412 and reactor powders synthesized under various conditions.

measurements manifests single exponential behavior for all four peaks (Table 2). Thus, we conclude there are four peaks in our ^{13}C NMR spectra and two-exponential behavior of deconvoluted peaks is explained by ^{13}C spin diffusion of long T_1 component to the short T_1 component rather than by two components. In general, properties of the peaks at 31.3, 32.8, and 34.1 ppm are not different from those of previously reported amorphous, orthorhombic crystalline, and monoclinic crystalline phases, respectively. The peak at 33.4 ppm has longer T_1 than the amorphous phase but shorter T_1 than the crystalline phases. Likewise, ^{13}C T_2 value of the peak at 33.4 ppm are between those of the amorphous phase and the crystalline phases. In contrast, T_{CH} of the peak is similar to those of crystalline phases. These results imply that the component for 33.4 ppm peak

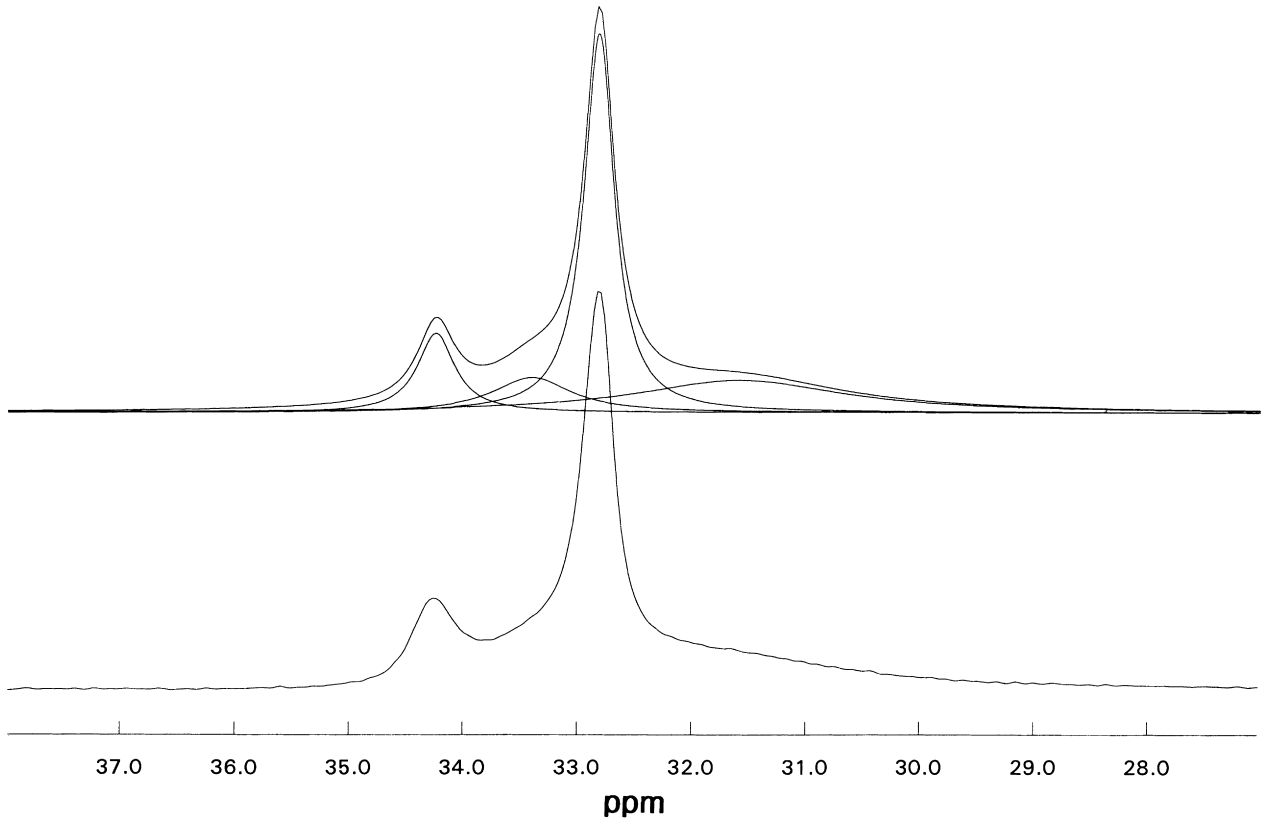

Fig. 14. Deconvoluted ^{13}C MAS spectrum for a typical UHMWPE, 30C_15P. Top: a simulated spectrum with each peak component, Bottom: experimental spectrum. Note that there is one more component at 33.4 ppm in addition to well-known three peaks from amorphous (at 31.3 ppm), orthorhombic crystalline (at 32.8 ppm), and monoclinic crystalline (at 34.1 ppm) phases.

has an intermediate dynamics between amorphous and crystalline phases or similar dynamic property to the crystalline phase depending on the observed dynamic frequency range. However, the component for the 33.4 ppm peak can be described to have the intermediate dynamic property in general. This 33.4 ppm component has somewhat different dynamic properties and chemical shift values from previously reported interfacial components [20] or crystalline-amorphous interphase [21]. Gammar-gauche effect [22] being considered, the chemical shift of 33.4 ppm bigger than 32.8 ppm suggests that this component is most likely to have all *trans* conformations. The chemical shift differences among 32.8, 33.4, and 34.1 ppm can be explained by molecular chain packing variation of each phase. The line width of the 33.4 ppm peak is also between those of the amorphous and crystalline phase peaks (Table 2), which could be just due to different T_2 relaxation times. Another possible reason could be that the chain packing in the component for 33.4 ppm peak is not as regular as those in the crystalline phases. Therefore, we assign this peak to an intermediate phase, which has all *trans* conformations but higher mobility than those of the crystalline phases. It is not certain at this moment that this intermediate phase is a transient phase between monoclinic and orthorhombic crystalline phases or between amorphous and crystalline phases. In either case, the intermediate phase of the peak at 33.4 ppm is expected to contribute to the non-crystalline halo in the X-ray diffraction data due to relatively poor packing of molecular chains. Further discussion on the peak assignment will be done with the results of variable temperature experiments later.

For comparison of morphological composition of each

Table 2
NMR parameter obtained from deconvoluted ^{13}C CPMAS NMR spectra of reactor samples and GUR412

NMR parameter	Amorphous (at 31.3 ppm)	Orthorhombic (at 32.8 ppm)	Monoclinic (at 34.1 ppm)	Intermediate (at 33.4 ppm)
$T_1(^{13}C)$	0.34–0.45 s	293–662 s 6.0–12 s	141–368 s 9.3–20 s	0.86–1.5 s
$T_2(^{13}C)$	0.43–0.83 ms	0.10–0.11 ms	0.094–0.11 ms	0.20–0.36 ms
T_{CH}	0.063–0.10 ms	0.032–0.043 ms	0.020–0.031 ms	0.017–0.038 ms
Line width	163–220 Hz	27–36 Hz	38–56 Hz	76–112 Hz

Table 3
Summary of phase composition in GUR412 and reactor samples obtained from ^{13}C MAS spectra without CP

Sample	Amorphous (at 31.3 ppm)	Orthorhombic (at 32.8 ppm)	Monoclinic (at 34.1 ppm)	Intermediate (at 33.4 ppm)
GUR412	0.347	0.446	0.062	0.145
10C_15P	0.169	0.640	0.099	0.092
30C_15P	0.252	0.488	0.151	0.109
90C_15P	0.201	0.677	0.049	0.072
30C_40P	0.216	0.473	0.155	0.157

sample, the MAS spectra were obtained with a very long pulse repetition delay of 1700 s and a pulse length of 30° flip angle but without CP. As listed in Table 3, more orthorhombic crystalline phase and less amorphous phase are present in our samples than the commercial sample GUR412. It is found that more monoclinic crystalline phase is formed in our reactor powders produced below 90°C than in GUR412 but not in the reactor powders made at 90°C. Less monoclinic and more orthorhombic crystalline phase is formed in the reactor powder samples produced at 90°C than at 30°C. The dependence of each phase content on the polymerization temperature determined by MAS NMR results are in good agreement with that of our X-ray diffraction data as shown in Fig. 7(a)). As discussed in the X-ray diffraction study section, the formation of the metastable monoclinic phase is less likely to take place at elevated polymerization temperatures.

For the study of the thermal behavior of newly synthesized UHMWPE reactor powders, CPMAS spectra at various temperatures are acquired and the results are summarized in Fig. 15. As a result of different CP efficiencies for different phases, CPMAS spectra cannot supply an accurate mass fraction of each phase. However, it is more convenient and timesaving to employ CPMAS than MAS spectra when relative mass fraction variation of each phase versus temperature is sufficient information for the thermal behavior study. In general, GUR412 sample shows somewhat different thermal behavior than reactor powders: with increasing temperature, (1) amorphous phase decreases initially but increases at higher temperatures ($T > 100$°C); and (2) orthorhombic crystalline and intermediate phases show some fluctuation but eventually decreases and increases, respectively; (3) monoclinic crystalline phase increases a little but decreases and disappears at higher temperature. Common tendency observed in our reactor samples is that monoclinic crystalline phase decreases and disappears eventually as temperature is raised. Another common behavior observed is that orthorhombic crystalline phase drops at temperatures higher than a certain point. Amorphous phase seems to stay constant in relative quantity. CPMAS spectra of samples annealed by slow cooling after the experiments at 120°C exhibit drastic depletion of monoclinic crystalline and intermediate phases and increase of orthorhombic crystalline phase (Fig. 15). By annealing, the amorphous phase is also reduced but not as drastic as the monoclinic crystalline phase. We plotted the data in different fashions in Fig. 16 to see the thermal behavior of each phase more clearly. In Fig. 16, the total quantity of the amorphous phase and intermediate phase in our reactor samples seems to increase, while the quantity of the amorphous phase alone stays constant at increasing temperature. We note that the temperature dependence of non-crystalline phases (sum of amorphous and intermediate phases) in the NMR experiments is consistent with that of the non-crystalline phase in X-ray diffraction experiments (Fig. 10). It should be reminded that 2θ values for the maximum of the non-crystalline halo for most UHMWPE powders in the X-ray diffraction analysis is about 20.5–21° which is clearly higher than the value of 19.4° associated with liquid-like amorphous molecules [11]. This implies that there is scattering contribution to the non-crystalline halo from some more tightly packed molecules, which are referred to as the intermediate phase in NMR analysis, than in the amorphous phase. The total amount of orthorhombic and monoclinic crystalline phases is reduced above 90°C, while the sum of the intermediate phase and the crystalline phases is almost constant as temperature is raised (Fig. 16 (c) and (d)). Our temperature dependent NMR and XRD data seem to indicate that in reactor powder samples monoclinic crystal phase is transformed to the orthorhombic crystal phase possibly via the intermediate phase in equilibrium with increasing temperature. The increased orthorhombic crystal phase is then transformed to the intermediate phase and eventually to the amorphous phase at higher temperatures. However, when the melted sample is slowly cooled, a large fraction of the amorphous phase is transformed to orthorhombic rather than back to the monoclinic crystalline or the intermediate phase. This result indicates that the monoclinic crystalline phase and the intermediate phase are metastable compared with the orthorhombic crystalline phase and that the intermediate phase plays a role as a transient phase between amorphous and orthorhombic crystalline phases. If a significant amount of the metastable monoclinic crystal phase is present at the solid state (as in our UHMWPE reactor powders synthesized at low temperatures), the intermediate phase may also play a role as a transient phase between the monoclinic and the orthorhombic crystalline phase at elevated temperatures.

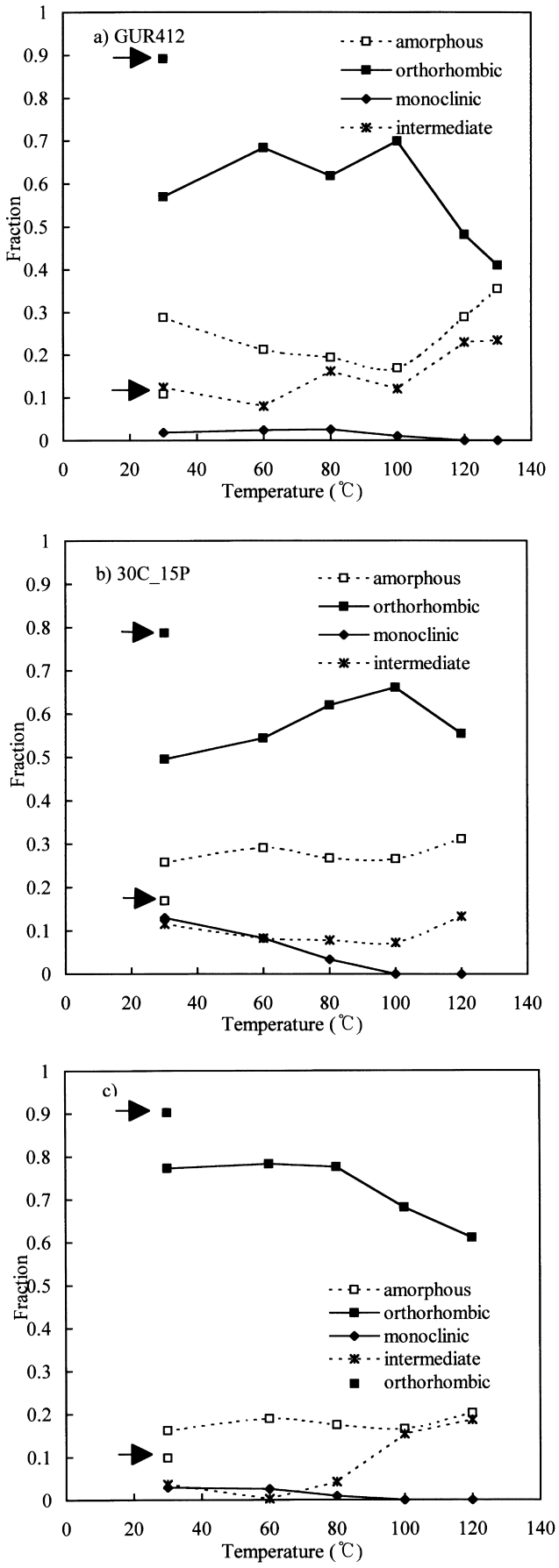

Fig. 15. Phase composition plots from CP/MAS spectra of each sample at various temperatures: (a) GUR412; (b) 30C_15P; and (c) 90C_15P. The arrows are pointed to the values for the composition of each sample at room temperature after annealing.

4. Conclusions

We have presented various characteristics of the nascent UHMWPE reactor powders prepared by polymerizing ethylene in the presence of soluble magnesium complexes under various reaction conditions. We have shown that the polymerization process applied in the study provides a high yield of UHMWPE even at low polymerization temperature, and the reactor powders exhibit high melting temperatures (137–143°C) and heat of melting (180–210 J/g). X-ray diffraction patterns and solid state ^{13}C MAS NMR spectra of the powders synthesized under various reaction conditions were examined and compared with those of a commercial UHMWPE powder. Our results revealed that a significant portion of the monoclinic phase is identified when the resin is polymerized at relatively low temperatures. Although the crystallinity of the newly synthesized powders was lower than that of the commercial UHMWPE (GUR412) at room temperature, temperature dependent XRD and NMR experiments showed that UHMWPE reactor powders exhibit different thermal behaviors from the commercial UHMWPE. This difference is shown to become more prominent with UHMWPE powders polymerized at low temperature in which a considerable amount of the metastable monoclinic crystal phase is produced.

In later reports, we will demonstrate that UHMWPE reactor powders synthesized in the study also have a distinct morphology characterized by a low bulk density, high micropore volume and inner surface area, and that these characters are essential to provide a successful continuous production of high strength, high modulus materials at temperature below their melting points [17]. In such solid state processing, the observation that the crystallinity and the crystal size of newly synthesized UHMWPE powders is increased at elevated temperatures (100–125°C) is important because solid state compaction of UHMWPE powders into coherent tapes is usually carried out at these temperatures. This increased crystal quality at 100–125°C as well as high ordering (non-entangled chain conformation) of the crystal phase appears to play an essential role in producing appropriate precursor tapes for higher strength and modulus products [17].

Acknowledgements

The authors wish to thank Dr Jung Yoon Do for preparing organic magnesium complexes used in the study. They also gratefully acknowledge Mr Tae Yoong Yeo for performing the X-ray diffraction measurements. Furthermore, Dr Jae Kap

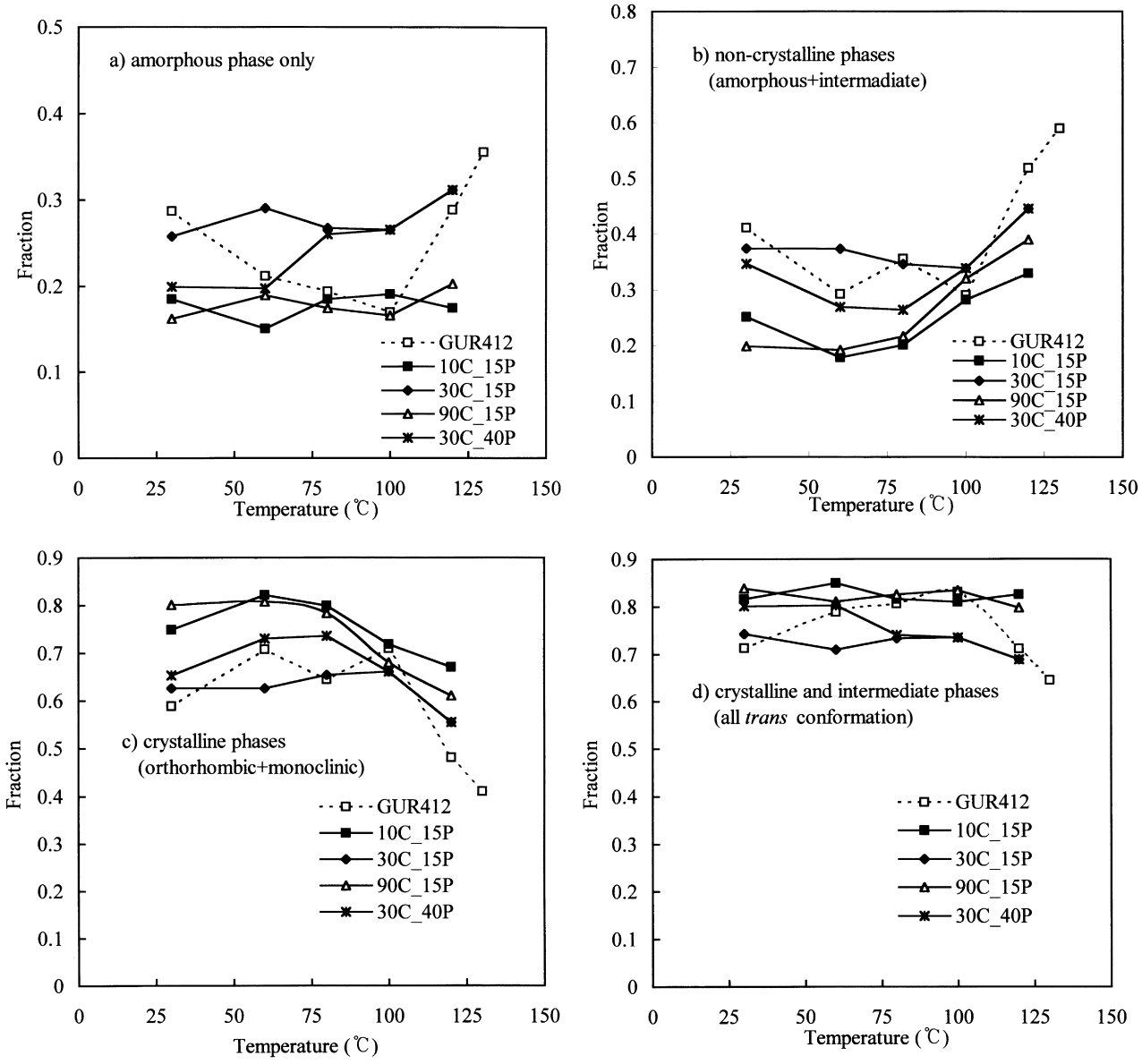

Fig. 16. Various combination of phase composition plots from CP/MAS spectra of each sample with increasing temperature: (a) amorphous phase only; (b) sum of amorphous and intermediate phases; (c) crystalline (sum of orthorhombic and monoclinic) phases; and (d) sum of crystalline and intermediate phases.

Jung at the Korea Basic Science Institute is thanked for deconvolution of NMR spectra.

References

[1] Birnkraut WH, Braun G, Falbe J. J Appl Polym Sci: Appl Polym Symp 1981;36:79.
[2] Chanzy H, Day A, Marchessault RH. Polymer 1967;8:567.
[3] Smith P, Chanzy HD, Rotzinger BP. Polym Commun 1985;26:258.
[4] Smith P, Chanzy HD, Rotzinger BP. J Mater Sci 1987;22:523.
[5] Rotzinger BP, Chanzy HD, Smith P. Polymer 1989;30:1814.
[6] Wang LH, Ottani S, Porter RS. Polymer 1991;32:1776.
[7] Seliknova VI, Zubov YA, Sinevich EA, Chvalun SN, Ivancheva NI, Smol'yanova OV, Ivanchev SS, Bakeev NF. Polym Sci USSR 1992;34:151.
[8] Won HY, Song JK, Joo YL, Lee HK, Park NC. Korean Patent KP98-15409, 1998.
[9] Russell KE, Hunter BK, Heyding RD. Polymer 1997;38:1409.
[10] Desper CR, Cohen SH, King AO. J Appl Polym Sci 1993;47:1129.
[11] Mcfaddin DC, Russell KE, Wu G, Heyding RD. J Polym Sci: Part B: Polym Phys 1993;31:175.
[12] Bennett AE, Rienstra C, Auger M, Lakshmi KV, Griffin RG. J Chem Phys 1995;103:6951.
[13] Torchia DAJ. Mag Res 1978;30:631.
[14] Bassett DC. Principles of polymer morphology. London: Cambridge University Press, 1981.
[15] Wunderlich B. Macromolecular physics: vol. 1 crystal structure, morphology, defects. London: Academic Press, 1973.
[16] Gedde UW. Polymer physics. London: Chapman & Hall, 1995.

[17] Joo YL, Lee HK, Song JK. J Appl Polym Sci, submitted for publication, 1999.
[18] Fu Y, Chen W, Pyda M, Londono D, Annis B, Boller A, Habenschuss A, Cheng J, Wunderlich B. J Macromol Sci-Phys 1996;B35:37.
[19] VanderHart DL, Khoury F. Polymer 1984;25:1489.
[20] Kitamaru R, Horri F, Murayama K. Macromolecules 1986;19:636.
[21] Kitamaru R, Horri F, Zhu Q, Bassett DC, Olley RH. Polymer 1994;35:1171.
[22] Tonneli AE. NMR spectroscopy and polymer microstructure: the conformational connection. New York: VCH Publisher, 1989.